

UC Irvine

ICTS Publications

Title

IL-6-induced skeletal muscle atrophy

Permalink

<https://escholarship.org/uc/item/719972x2>

Journal

Journal of Applied Physiology, 98(3)

ISSN

8750-7587 1522-1601

Authors

Haddad, F.
Zaldivar, F.
Cooper, D. M
et al.

Publication Date

2005-03-01

DOI

10.1152/jappphysiol.01026.2004

Copyright Information

This work is made available under the terms of a Creative Commons Attribution License, available at <https://creativecommons.org/licenses/by/4.0/>

Peer reviewed

IL-6-induced skeletal muscle atrophy

F. Haddad,¹ F. Zaldivar,² D. M. Cooper,² and G. R. Adams¹

Departments of ¹Physiology and Biophysics and ²Pediatrics, University of California, Irvine, California

Submitted 16 September 2004; accepted in final form 4 November 2004

Haddad, F., F. Zaldivar, D. M. Cooper, and G. R. Adams. IL-6-induced skeletal muscle atrophy. *J Appl Physiol* 98: 911–917, 2005. First published November 12, 2004; doi:10.1152/jappphysiol.01026.2004.—Chronic, low-level elevation of circulating interleukin (IL)-6 is observed in disease states as well as in many outwardly healthy elderly individuals. Increased plasma IL-6 is also observed after intense, prolonged exercise. In the context of skeletal muscle, IL-6 has variously been reported to regulate carbohydrate and lipid metabolism, increase satellite cell proliferation, or cause muscle wasting. In the present study, we used a rodent local infusion model to deliver modest levels of IL-6, comparable to that present after exercise or with chronic low-level inflammation in the elderly, directly into a single target muscle in vivo. The aim of this study was to examine the direct effects of IL-6 on skeletal muscle in the absence of systemic changes in this cytokine. Data included cellular and molecular markers of cytokine and growth factor signaling (phosphorylation and mRNA content) as well as measurements to detect muscle atrophy. IL-6 infusion resulted in muscle atrophy characterized by a preferential loss of myofibrillar protein (–17%). IL-6 induced a decrease in the phosphorylation of ribosomal S6 kinase (–60%) and STAT5 (–33%), whereas that of STAT3 was increased approximately two-fold. The changes seen in the IL-6-infused muscles suggest alterations in the balance of growth factor-related signaling in favor of a more catabolic profile. This suggests that downregulation of growth factor-mediated intracellular signaling may be a mechanism contributing to the development of muscle atrophy induced by elevated IL-6.

suppressor of cytokine signaling; signal transducer activator of transcription; insulin-like growth factor I; 70-kDa ribosomal S6 kinase

IL-6 IS AN intercellular signaling molecule traditionally associated with the control and coordination of immune responses. With regard to skeletal muscle, the elevation of “proinflammatory” cytokines such as IL-6 is generally viewed in the context of potentially deleterious impacts. For example, there are observations that IL-6 either directly or indirectly mediates catabolic effects on skeletal muscle (23). In a broader context, IL-6 appears to be related to growth deficits in children in several disease states (e.g., Ref. 9) and to the process of sarcopenia in the elderly (7, 26). It seems somewhat paradoxical then that a putative positive stress, exercise, can include a significant production of proinflammatory cytokines such as IL-6 (e.g., Refs. 39, 41, 44, 49).

Recently, some investigators have suggested that elevations in IL-6 in response to exercise may play an anti-inflammatory role, principally by inhibiting the production of TNF- α , a prototypical inflammatory mediator (42). In addition, IL-6 has been shown to participate in metabolic control pathways during exercise (20, 43, 48, 49). Clearly, these roles appear to be at

variance with the traditional view of IL-6 as a catabolic agent in skeletal muscle.

The growth hormone (GH)-insulin-like growth factor (IGF)-I axis is a critical mediator of skeletal muscle growth and adaptation (11, 45). In the context of whole body growth regulation, IGF-I functions under the control of GH (45). With regard to compensatory muscle adaptation, autocrine/paracrine IGF-I has been shown to regulate aspects of the compensatory adaptation of skeletal muscle as well as muscle growth and development (e.g., Refs. 2–5, 27, 28). We recently reported that locally (e.g., within a single muscle) elevated levels of GH can stimulate the development of skeletal muscle hypertrophy in vivo and that this response is most likely mediated by IGF-I (3).

In addition to production by immune cells, IL-6 is also synthesized by nonimmune cell types and may exert biologically significant effects on a variety of tissues, including muscle, even in the absence of overt pathological conditions (13, 20). A number of studies have indicated that IL-6 can interfere with the GH-IGF-I axis (9, 36). However, the mechanism of this interference has not been established.

The experiments described in this report stem from recent work indicating that there is potential for convergence of elements associated with both IL-6 and GH-IGF-I axis signaling (6, 25, 30, 31, 40, 50, 56, 57). These common elements include signaling via the Janus kinase (JAK)-signal transducer activator of transcription (STAT) pathway (21, 30, 50) (Fig. 1).

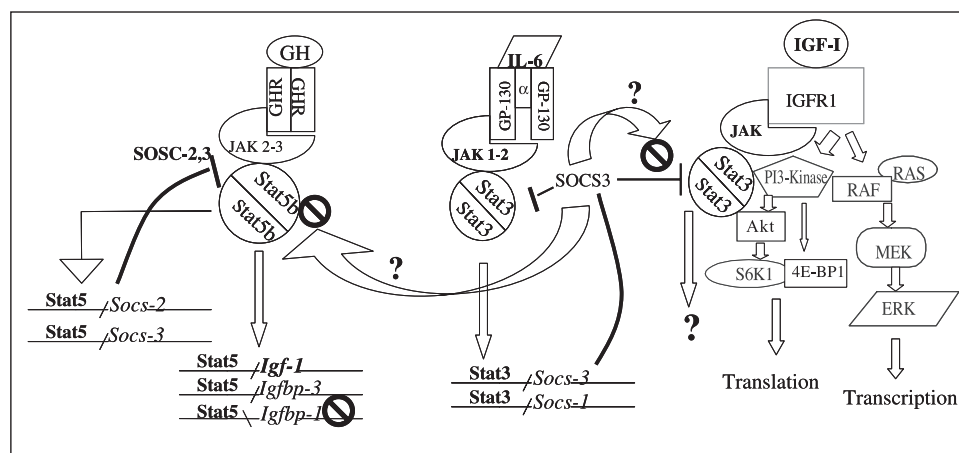
A critical outcome of JAK/STAT activity is the translocation of STAT to the nucleus, leading to alterations in the transcription and expression of a number of proteins. In the context of cytokine-growth factor interactions, one of the more significant changes may be alterations in the expression of members of the suppressors of cytokine signaling (SOCS) family (6, 47). SOCS family proteins can act as the negative regulators of JAK/STAT signaling, thereby affecting STAT activity.

The working hypothesis for the present experiments was that IL-6 may interact with JAK/STAT signaling pathways, leading to changes in SOCS expression, and that this process may lead to a decrease in signaling associated with the GH and/or IGF-I receptors. Based on the literature, the potential for IL-6-mediated interference with growth factor signaling has been diagrammed in Fig. 1. These experiments were designed to determine to what extent and how moderate physiological levels of IL-6, such as those seen after exercise, may activate or suppress signaling to produce an integrated cellular response. The overall goal of this line of research was to examine the potential for a novel role of the cytokine/growth factor interactions as they impact muscle growth and the anabolic adaptation to exercise.

Address for reprint requests and other correspondence: G. R. Adams, Associate Researcher, Dept. of Physiology & Biophysics, Univ. of California, Irvine, Medical Sciences 1, Rm. D335, Irvine, CA 92697-4560 (E-mail: GRAdams@uci.edu).

The costs of publication of this article were defrayed in part by the payment of page charges. The article must therefore be hereby marked “advertisement” in accordance with 18 U.S.C. Section 1734 solely to indicate this fact.

Fig. 1. Potential interactions of signaling elements serving the growth hormone (GH), IL-6, and insulin-like growth factor (IGF)-I receptors. MEK, mitogen-activated protein kinase kinase; JAK, Janus kinase; GHR, GH receptor; RAS, renin-angiotensin system; SOCS, suppressors of cytokine signaling; IGFBP, IGF binding protein.



METHODS

Sixteen female Sprague-Dawley rats weighing 263 ± 5 g were randomly assigned to normal control ($n = 5$), saline-infused (Sal; $n = 5$), or IL-6 infusion (IL-6; $n = 6$) groups. All procedures were approved by the University of California, Irvine, Institutional Animal Care and Use Committee.

Local infusion. The local infusion protocol used in this study has been described in previous publications (3, 28). Infusion was accomplished via a catheter (0.006 in. inner diameter, Teflon, Cole-Parmer) attached to a mini-osmotic pump (Alzet model 2002, Alza). The mini-osmotic pumps were filled under aseptic conditions following the manufacturer's instructions. For catheter implantation, the rats were anesthetized with ketamine/acepromazine (80/2 mg/kg), and incisions were made in the skin overlying the tibialis anterior (TA) muscle (~1.5-cm incision) and on the back (~0.5-cm incision). Two small cuts (~1 mm) were made in fascia of the TA muscle using iris scissors. One cut was near the proximal end of the muscle, whereas the other was distal, near the tendon. The catheter was tunneled under the fascia and secured in place with sutures (4-0 Ethicon). The proximal end of the catheter was tunneled under the skin to the back incision. The catheter was filled with the same solution as the pumps, and the distal end of the catheter was closed by tying off with 2-0 suture. The proximal end of the catheter was then mated with the osmotic pump, which had been primed by preincubation in sterile saline at 37°C. The pump was then placed under the skin via the back incision, and both incisions were closed. At the termination of the infusion protocols, the osmotic pumps were removed, and any remaining infusate was aspirated via a syringe to verify pump function.

On determination that the infusion protocol per se had no effect on skeletal muscle, the majority of the comparisons were made between the infused (IL-6) and contralateral (Contra) muscles from the same animals. The normal control and Sal animals were used to evaluate the potential for IL-6 impacts at the level of the whole animal (e.g., body mass, heart weight, plasma IL-6) and individual muscle mass. Previous work has demonstrated that the local infusion of vehicle per se does not result in changes to infused muscles (Refs. 3, 12; G. R. Adams unpublished observations). The normal control group animals did not undergo pump implantation or any surgical intervention. The Sal rats experienced the same procedures as the IL-6-infused animals, with the exception that IL-6 was excluded from the muscle infusate. The Sal group was included to reconfirm that vehicle infusion had no effect on muscle mass.

A third group of three rats was implanted for IL-6 infusion and then killed at 3 days postsurgery to evaluate the potential for short-term systemic effects of the implantation and infusion protocol.

IL-6 dose determination. The dose of IL-6 selected for this study was based on recent observations of exercise-induced IL-6 increases

in humans (48). In that study, Steensberg et al. reported that plasma IL-6 concentrations reached 22 ng/l after strenuous exercise (48). Our interest was to determine whether similar levels of IL-6 would impact skeletal muscle homeostasis in rats. Assuming a blood volume of ~16 ml in ~250-g rats (19), an equivalent systemic dose of IL-6 would be 0.352 ng. For this study, the concentration of IL-6 loaded in the pumps was designed to provide $0.7 \text{ pg} \cdot \text{muscle}^{-1} \cdot \text{h}^{-1}$ (whole body dose scaled to TA muscle mass). Vehicle consisted of 0.9% saline. It is important to note that this IL-6 dose is many times lower than would be used for sepsis-related studies (38, 53).

Tissue collection and analysis. Fourteen days after the implantation surgeries, rats were killed using Pentosol euthanasia solution. The TA and extensor digitorum longus muscles of both the infused and Contra leg were removed, weighed, snap frozen, and stored at -80°C for later analysis.

Muscle protein was determined from whole muscle homogenates using the biuret method (24). Total muscle protein was calculated from the product of the concentration and the wet weight of the muscle sample recorded at death. Total myofibrillar protein was determined as previously described using a modification of the method of Solaro et al. (28, 46, 52).

DNA determination. DNA concentration was measured in whole muscle homogenates using a fluorometric assay for the DNA binding fluorochrome bisbenzimidazole H-33258 (Calbiochem, San Diego, CA). Calf thymus DNA was used as a standard (34).

Total RNA isolation. Total RNA was extracted from preweighed frozen muscle samples using the TRI Reagent (Molecular Research Center, Cincinnati, OH), according to the company's protocol, which is based on the method described by Chomczynski and Sacchi (15). Extracted RNA was precipitated from the aqueous phase with isopropanol and, after being washed with ethanol, was dried and suspended in a known volume of nuclease-free water. The RNA concentration was determined by optical density at 260 nm (using an OD260 unit equivalent to $40 \mu\text{g/ml}$). The muscle total RNA concentration is calculated based on total RNA yield and the weight of the extracted muscle piece. The RNA samples were stored frozen at -80°C to be used subsequently in determining the specific mRNA expression using relative RT-PCR procedures.

Reverse transcription. One microgram of total RNA was reverse transcribed for each muscle sample using the SuperScript II RT from GIBCO and a mix of oligo dT (100 ng/reaction) and random primers (200 ng/reaction) in a 20- μl total reaction volume at 45°C for 50 min, according to the provided protocol. At the end of the reverse transcription reaction, the tubes were heated at 90°C for 5 min to stop the reaction and then stored at -80°C until used in the PCR reactions for specific mRNA analyses.

PCR. As described previously (1, 27, 28, 55), relative RT-PCR method using 18S as internal standard (Ambion, Austin, TX) was applied to study the expression of specific mRNAs of interest, including SOCS-2, SOCS-3, Atrogin-1, MURF-1, and IGF-I. Primers were purchased from Life Technology, GIBCO. We have previously published the sequence for the IGF-I primers (27). All other primers used are provided in Table 1. All primers were tested for their compatibility with the alternate 18S primers.

In each PCR reaction, 18S ribosomal RNA was coamplified with the target cDNA (mRNA) to serve as an internal standard and to allow correction for differences in starting amounts of total RNA. The 18S primers were mixed with competitors at an optimized ratio that could range from 1:4 to 1:10 to bring down the 18S signal, which allows its linear amplification to the same range as the coamplified target mRNA (Ref. 10; Ambion, relative RT-PCR kit protocol).

For each specific target mRNA, the reverse transcription and PCR reactions were carried out under identical conditions using the same reagent premix for all of the samples to be compared in the study. To validate the consistency of the analysis procedures, at least one representative from each group was included in each RT-PCR run.

Amplifications were carried out in a Stratagene Robocycler with an initial denaturing step of 3 min at 96°C, followed by 25 cycles of 1 min at 96°C, 1 min at 55°C (55–60°C depending on primers), 1 min at 72°C, and a final step of 3 min at 72°C. PCR products were separated on a 2–2.5% agarose gel by electrophoresis and stained with ethidium bromide, and signal quantification was conducted by laser scanning densitometry, as reported previously (55). In this approach, each specific mRNA signal is normalized to its corresponding 18S. For each primer set, PCR conditions (cDNA dilutions, 18S competitor/primer mix, MgCl₂ concentration, and annealing temperature) were set to optimal conditions so that both the target mRNA and 18S product yields are in the linear range of the semilog plot when the yield is expressed as a function of the number of cycles (10).

Phosphorylation state of intracellular signaling proteins. The phosphorylation state of STAT3, STAT5, and p70-S6 kinase (S6K1) were examined by immunoblotting using phospho-specific antibodies (Cell Signaling Technology), as reported previously (1, 27). Muscle samples were extracted by homogenization in seven volumes of ice-cold buffer A [50 mM Tris·HCl, pH 7.8, 2 mM potassium phosphate, 2 mM EDTA, 2 mM EGTA, 50 mM β-glycerophosphate, 10% glycerol, 1% Triton X-100, 1 mM DTT, 3 mM benzamide, 1 mM sodium orthovanadate, 10 μM leupeptin, 5 μg/ml aprotinin, 200 μg/ml soybean trypsin inhibitor, and 1 mM 4-(2-aminoethyl)-benzene-sulphonyl fluoride] using a motor-driven glass pestle. The homogenate was immediately centrifuged at 12,000 g for 30 min at 4°C. The supernatant was immediately saved in aliquots at –80°C for subsequent use in immunoblotting. The supernatant protein concentration was determined using the Bio-Rad protein assay with BSA as standard. Approximately 50 μg of supernatant proteins were subjected to SDS-PAGE, then electrophoretically transferred to a polyvinylidene difluoride membrane (Immobilon-P) using 10% methanol, 1 mM orthovanadate, 25 mM Tris, and 193 mM glycine, pH 8.3. Antibodies

Table 1. *SOCS primers*

Target mRNA	PCR Primer Sequence 5'→3'	Product Size, bp	GeneBank Acc. No.
SOCS-3	Fwd: GGGGCCCTCCTTCTCTTTAC	238	AF075383
	Rev: GCAGCTGGGTCACTTTCTCATAGG		
SOCS-2	Fwd: CGAAGCCCTGCGTGAGC	207	AF075382
	Rev: ATCTGAATTTCCCGTCTTGTA		
Atrogin	Fwd: CAGAACAGCAAAACCAAACTC	218	NM_133521
	Rev: GCGATGCCACTCAGGGATGT		
MURF-1	Fwd: TACCGAGAGCAGTTGGAAAGT	215	AY059627
	Rev: CTCAAGGCCTCTGCTATGTGTT		

SOCS, Suppressor of cytokine signaling; Fwd, forward; Rev, reverse.

Table 2. *Somatic/systemic effects of local IL-6 infusion*

Group	Body Mass, g	Heart Mass, mg/g body wt	Plasma IL-6, pg/ml
Control	271 ± 12	2.9 ± 0.1	10.7 ± 1.9
IL-6 infused	280 ± 3	3.0 ± 0.2	7.6 ± 2.2

were detected using the enhanced chemiluminescence method of detection (Amersham). Signal intensity was determined by laser-scanning densitometry (Molecular Dynamics). For each specific antibody, all samples were run under identical (previously optimized) conditions, including the transfer on the membrane, the reaction with the primary and secondary antibodies, washing conditions, enhanced chemiluminescence detection, and film exposure. If more than one gel run was required, at least one representative sample from each group was included to ensure the consistency of this analysis. In addition, a positive control, provided by the antibody manufacturer, was run on each gel to allow for normalization. For each set of Western blotting and detection conditions, the detected signal was directly proportional to the amount of protein loaded on the gel over a range of 20–150 μg (data not shown).

As reported previously, total protein levels of STAT3, STAT5, and S6K1 were assessed using nonphospho-specific immunoblots to ensure that the level of protein had not decreased to a point where it could become limiting (1, 27). However, because these processes are highly regulated and not dependent on mass action (i.e., driven by availability of substrate), the results are expressed in terms of the change in phosphorylation state rather than a ratio of the nonphospho to total protein ratio. In some circumstances, the use of such ratio data would obscure important changes in regulatory events.

Plasma IL-6. Plasma IL-6 was measured via ELISA (R&D Systems), essentially as described previously (39).

Statistical analysis. All values are reported as means ± SE. Differences between the Contra and treatment (IL-6) muscles were determined by *t*-test using the PRISM software package (Graphpad). Pearson's correlation analysis was used to assess the relationship between SOCS-3 mRNA and total or myofibrillar protein content using the Prism software package. For all statistical tests, the 0.05 level of confidence was accepted for statistical significance.

RESULTS

No systemic or somatic impacts of IL-6 infusion protocol. Fourteen days of IL-6 infusion had no effect on the body mass or the mass of the heart (Table 2). The low dose and efficient clearance of IL-6 prevented systemic impacts, such that effects were limited to the target muscle since the underlying extensor digitorum longus was not affected. Compared with untreated control animals, the plasma levels of IL-6 in the local infusion rats were not different (Table 2). This is not a particularly surprising finding considering the low dose used in this study (e.g., 0.7 pg·muscle⁻¹·h⁻¹, equivalent to 2.8 pg/kg body mass). Unchanged plasma IL-6 levels indicate that neither the locally infused IL-6 nor the catheter implantation per se impacted the plasma IL-6 levels.

In a separate group of three animals, IL-6 infusion was carried out for 3 days to determine whether the catheter implantation process per se resulted in short-term alterations in plasma IL-6. The plasma levels of IL-6 in this acute group were not different from those of the nontreatment control group (10.7 ± 1.9 control vs. 9.6 ± 3.0 pg/ml acute IL-6 infused).

Catabolic effects of local IL-6 infusion. As reported previously (3, 12), vehicle infusion had no effect on the mass, protein concentration, or protein content of rat skeletal mus-

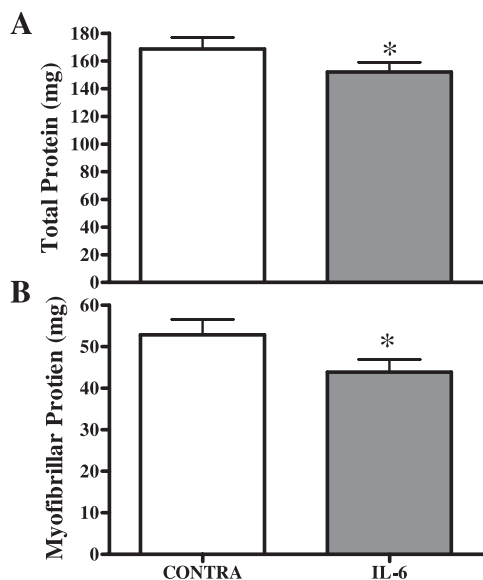


Fig. 2. IL-6-induced muscle atrophy. Infusion of IL-6 resulted in a decrease in muscle total (A) and myofibrillar fraction (B) protein content. Contra, contralateral muscle; IL-6, IL-6-infused muscle. * $P < 0.05$ vs. Contra.

cles. For example, the protein content of the muscles was (in mg) 166.2 ± 4.3 , 165.8 ± 3.4 , and 167.1 ± 3.8 for the normal control, Contra Sal, and Sal muscles, respectively. In contrast, IL-6 infusion resulted in significant atrophy of the infused TA muscles (vs. Contra), as evidenced by a 9% decrease in total protein content (168.4 ± 8 vs. 152.1 ± 7 mg; Fig. 2A) and a 17% decrease in myofibrillar protein (Fig. 2B). The underlying extensor digitorum longus muscles were unaffected by the IL-6 infused into the TA (data not shown).

Intracellular signaling and elevated IL-6. Infusion IL-6 resulted in an increase in the phosphorylation state of STAT3 (Fig. 3C) and a decrease in the phosphorylation of STAT5 (Fig. 3D). There was no change in the total amount of STAT3 detected by immunoblot (Contra: 832 ± 80 mg vs. IL-6: 726 ± 95 mg). The total amount of STAT5 protein was significantly increased in the IL-6-infused muscles (Contra: 455 ± 49 mg vs. IL-6: 651 ± 54 mg).

Compared with the Contra muscles, IL-6 infusion resulted in a significant increase in the expression and/or accumulation of the mRNA for SOCS-3 (Fig. 4) but had no impact on the levels of SOCS-2 mRNA detected in these muscles (0.18 ± 0.015 vs. 0.18 ± 0.018).

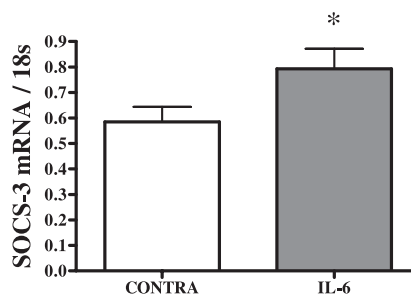


Fig. 4. IL-6-induced changes in SOCS-3 mRNA. IL-6 infusion resulted in an increase in the expression and/or accumulation of the mRNA for SOCS-3. * $P < 0.05$ vs. Contra.

Relative to the Contra muscle, the phosphorylation of S6K1 was decreased in IL-6-infused muscles (Fig. 5). There was no change in the total amount of S6K1 detected by immunoblot (Contra: 594 ± 41 mg vs. IL-6: 647 ± 48 mg).

IL-6 infusion resulted in a significant increase in the mRNA for IGF-I in the IL-6-infused muscles (Fig. 6).

There were no significant differences between the Contra and IL-6-infused muscles in the expression of the mRNA for Atrogin-1 (0.19 ± 0.017 vs. 0.22 ± 0.029 , respectively) or MURF-1 (0.37 ± 0.038 vs. 0.41 ± 0.037 , respectively).

DISCUSSION

A number of apparently contrasting roles, ranging from anabolic to catabolic and metabolic regulation, have been described for IL-6 and its interactions with skeletal muscle (7, 20, 23, 26, 42, 43, 48, 49). The fact that elevated IL-6 can be a feature of such a wide variety of conditions, including disease, aging, and participation in intense exercise, indicates that a clear understanding of the direct effects of this cytokine on muscle is of utmost importance. To our knowledge, this is the first study to examine the effects of a relatively modest dose of IL-6 on skeletal muscle in the absence of somatic level alterations that would be expected to occur with systemic elevation of this cytokine.

IL-6-induced muscle atrophy. Although elevated IL-6 levels have often been associated with a catabolic state in skeletal muscle, most of these observations were made in the presence of complex conditions, such as sepsis, experimentally induced inflammation, or cachexia (e.g., Refs. 8, 9, 22, 35), or via greatly elevated systemic IL-6 with potential indirect effects (23, 36, 38, 53). In the present study, we have demonstrated

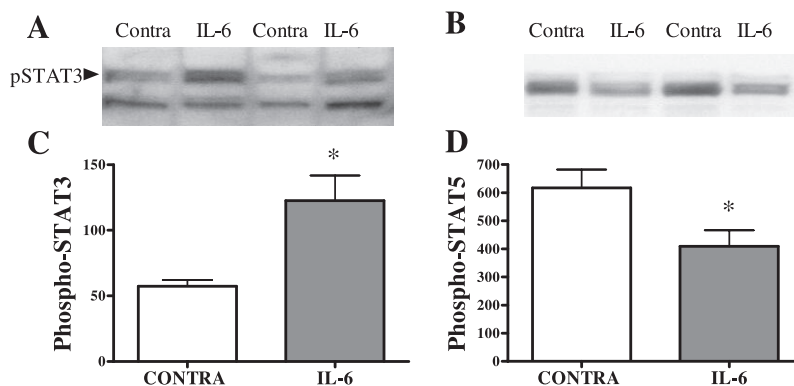


Fig. 3. IL-6-induced changes in STAT phosphorylation. Representative immunoblot results are presented for phospho-STAT3 (A) and phospho-STAT5 (B). IL-6 infusion resulted in an increase in the phosphorylation of STAT3 (C) and a decrease in the phosphorylation of STAT5 (D). * $P < 0.05$ vs. Contra.

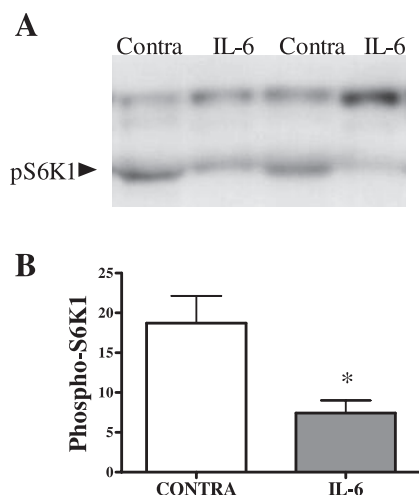


Fig. 5. IL-6-induced changes in p70-S6 kinase (S6K1) phosphorylation. *A*: representative immunoblot is presented for phospho-S6K1. *B*: IL-6 infusion resulted in a decrease in the amount of phosphorylated S6K1 protein. * $P < 0.05$ vs. Contra.

that, in the absence of systemic effects, IL-6 can directly induce skeletal muscle atrophy in otherwise healthy rats. Our data also indicate that IL-6 disproportionately affected the myofibrillar protein compartment, suggesting that this treatment would have meaningful functional impacts.

IL-6 intracellular signaling. Receptor-induced phosphorylation of STATs via the JAK tyrosine kinases leads to STAT activation (30). Activated STATs dimerize and are translocated to the nucleus and participate in transcriptional regulation (30).

The phosphorylation of STAT3, which is generally reported to be the primary STAT activated by ligation of the IL-6 receptor (6, 14, 30), was significantly elevated in the IL-6-infused muscles (Fig. 3C). Interestingly, the IL-6-infused muscles experienced a concomitant decrease in STAT5 phosphorylation (Fig. 3D). In some tissues, STAT5 phosphorylation is associated with the activity of the GH receptor (16–18, 21). These results may represent a form of complementary inhibition. That is, increased signaling via the IL-6 receptor (STAT3) may feed back via SOCS-3 and inhibit signaling via another, possibly growth factor-related, receptor-mediated pathway (e.g., STAT5).

The increase in SOCS-3 mRNA seen in the IL-6-infused muscles is most likely a result of the increased STAT3 activity (Figs. 3C and 4). SOCS-3 is known to mediate downregulation of signaling via the IL-6 receptor (6). However, there are

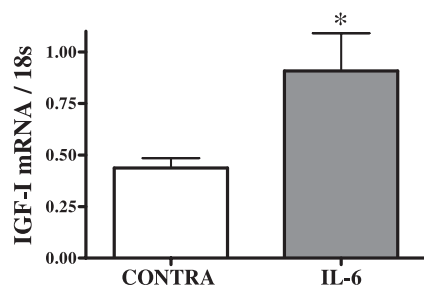


Fig. 6. IL-6-induced changes in IGF-I mRNA. IL-6 infusion resulted in increased expression and/or accumulation of the mRNA for IGF-I. * $P < 0.05$ vs. Contra.

reports that SOCS-3 can feed back on JAK/STAT activity of both the GH and IGF-I receptors as well (14, 25, 36). Based on their results in a growth-retarded, IL-6-overexpressing mouse, Lieskovska et al. (37) indicated that the observed increase in SOCS-3 mRNA suggests that SOCS-3 is the most likely agent attenuating GH signaling. Conversely, Woelfle and Rotwein (54) recently demonstrated that GH-related STAT5 signaling regulates SOCS-1 and -2 but has no effect on SOCS-3 expression.

In support of a potential mechanistic role of IL-6 signaling-induced changes in SOCS-3 in the atrophy process, there were significant negative correlations between SOCS-3 mRNA and both total and myofibrillar protein content in the muscles from this study (Fig. 7). This suggests that the changes in SOCS-3 mRNA most likely resulted in alterations at the protein level and that this agent was modulating functionally significant processes within skeletal muscle.

Mechanisms of IL-6-mediated catabolic activity. We have recently demonstrated that increased S6K1 phosphorylation is induced by IGF-I infusion and is associated with the development of skeletal muscle hypertrophy (28). The S6K1 protein is phosphorylated by a number of kinases, notably as part of the phosphoinositol 3-kinase signaling pathway. Phosphorylation of S6K1 is associated with an increase in translation and is known to occur with increased muscle loading, most likely subsequent to IGF-I receptor ligation (27, 28, 32). The primary impact of S6K1 activity on translation appears to be related to increases in the translation of specific mRNAs that encode components of the translational apparatus itself (29, 51). Relative to the Contra muscle, the phosphorylation of S6K1 was decreased in IL-6-infused muscles (Fig. 6). A decline in S6K1 phosphorylation may indicate that one of the catabolic impacts of elevated IL-6 is a decrease in translational capacity.

In contrast to an apparent decrease in IGF-I-related signaling (i.e., phospho-S6K1), we detected a significant increase in the mRNA for IGF-I in the IL-6-infused muscles (Fig. 6). This most likely represents GH-independent (and therefore non-STAT5 dependent), autocrine/paracrine induction of IGF-I.

We have generally found that changes in muscle IGF-I mRNA parallel alterations in muscle IGF-I peptide levels (e.g.,

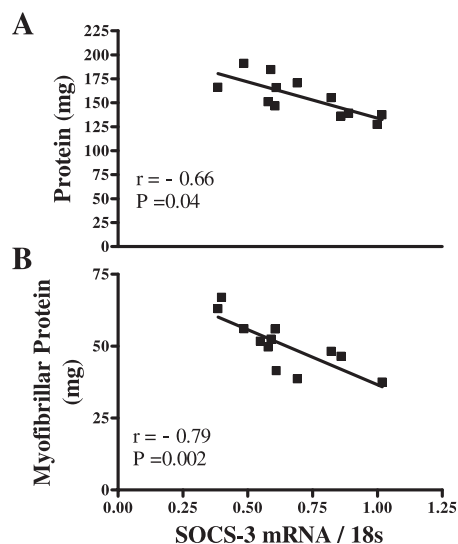


Fig. 7. Relationship between SOCS-3 expression and muscle protein. SOCS-3 mRNA levels were negatively correlated with the muscle content of total protein (*A*) and with the muscle content of myofibrillar protein (*B*).

Ref. 2). In the present context, a decrease in IGF-I-mediated signaling in conjunction with an attempt to increase autocrine/paracrine IGF-I production might suggest that IL-6-mediated interference with downstream components related to IGF-I signaling may be stimulating an increase in IGF-I as a compensatory response.

The mRNAs for the E3-ubiquitin-protein ligases atrogin-1 and MURF-1 did not change significantly in response to IL-6 infusion. This indicates that IL-6 does not appear to mediate muscle atrophy via pretranslational modulation of these proteins.

In summary, in this study, we delivered relatively modest levels of IL-6, such as those that might be present after exercise (48) or with chronic low-level inflammation in the elderly (7, 26), directly into a single target muscle in vivo. This dose of IL-6, which was undetectable in the systemic circulation, resulted in significant muscle atrophy. The cellular and molecular changes seen in the IL-6-infused muscles suggest that negative feedback mechanisms (SOCS) were activated, altering the balance of STAT protein phosphorylation in favor of a more catabolic profile. This suggests that downregulation of growth factor-mediated intracellular signaling may be a mechanism contributing to the development of muscle atrophy induced by chronically elevated IL-6.

ACKNOWLEDGMENTS

The authors thank Ming Zeng and Li-Ying Zhang for technical assistance.

GRANTS

This work was supported by National Institute of Arthritis and Musculoskeletal and Skin Diseases Grant AR-45594.

REFERENCES

- Adams GR, Caiozzo VJ, Haddad F, and Baldwin KM. Cellular and molecular responses to increased skeletal muscle loading after irradiation. *Am J Physiol Cell Physiol* 283: C1182–C1195, 2002.
- Adams GR and Haddad F. The relationships between IGF-1, DNA content, and protein accumulation during skeletal muscle hypertrophy. *J Appl Physiol* 81: 2509–2516, 1996.
- Adams GR and McCue SA. Localized infusion of IGF-I results in skeletal muscle hypertrophy in rats. *J Appl Physiol* 84: 1716–1722, 1998.
- Adams GR, McCue SA, Bodell PW, Zeng M, and Baldwin KM. Effects of spaceflight and thyroid deficiency on hindlimb development. I. Muscle mass and IGF-I expression. *J Appl Physiol* 88: 894–903, 2000.
- Adams GR, McCue SA, Zeng M, and Baldwin KM. The time course of myosin heavy chain transitions in neonatal rats: importance of innervation and thyroid state. *Am J Physiol Regul Integr Comp Physiol* 276: R954–R961, 1999.
- Alexander WS. Suppressors of cytokine signaling (SOCS) in the immune system. *Nat Rev Immunol* 2: 410–416, 2002.
- Barbieri M, Ferrucci L, Ragno E, Corsi A, Bandinelli S, Bonafe M, Olivieri F, Giovagnetti S, Franceschi C, Guralnik JM, and Paolisso G. Chronic inflammation and the effect of IGF-I on muscle strength and power in older persons. *Am J Physiol Endocrinol Metab* 284: E481–E487, 2003.
- Barton BE. IL-6-like cytokines and cancer cachexia: consequences of chronic inflammation. *Immunol Res* 23: 41–58, 2001.
- Benedetti F, Alonzi T, Moretta A, Lazzaro D, Costa P, Poli V, Martini A, Ciliberto G, and Fattori E. Interleukin 6 causes growth impairment in transgenic mice through a decrease in insulin-like growth factor-1. *J Clin Invest* 99: 643–650, 1997.
- Bickel CS, Slade JM, Haddad F, Adams GR, and Dudley GA. Acute molecular responses of skeletal muscle to resistance exercise in able-bodied and spinal cord-injured subjects. *J Appl Physiol* 94: 2255–2262, 2003.
- Butler AA and LeRoith D. Control of growth by the somatotropic axis: growth hormone and the insulin-like growth factors have related and independent roles. *Annu Rev Physiol* 63: 161–164, 2001.
- Chakravarthy MV, Davis BS, and Booth FW. IGF-I restores satellite cell proliferative potential in immobilized old skeletal muscle. *J Appl Physiol* 89: 1365–1379, 2000.
- Chargé SBP, Brack AS, and Hughes SM. Aging-related satellite cell differentiation defect occurs prematurely after Ski-induced muscle hypertrophy. *Am J Physiol Cell Physiol* 283: C1228–C1241, 2002.
- Chen E, Gadina M, Chen M, and O'Shea JJ. Advances in cytokine signaling: the role of Jaks and STATs. *Transplant Proc* 31: 1482–1487, 1999.
- Chomczynski P and Sacchi N. Single step method of RNA isolation by acid guanidinium thiocyanate-phenol-chloroform extraction. *Anal Biochem* 162: 156–159, 1987.
- Chow JC, Ling PR, Qu Z, Laviola L, Ciccarone A, Bistrrian BR, and Smith RJ. Growth hormone stimulates tyrosine phosphorylation of JAK2 and STAT5, but not insulin receptor substrate-1 or SHC proteins in liver and skeletal muscle of normal rats in vivo. *Endocrinology* 137: 2880–2886, 1996.
- Davey HW, McLachlan MJ, Wilkins RJ, Hilton DJ, and Adams TE. STAT5b mediates the GH-induced expression of SOCS-2 and SOCS-3 mRNA in the liver. *Mol Cell Endocrinol* 158: 111–116, 1999.
- Davey HW, Xie T, McLachlan MJ, Wilkins RJ, Waxman DJ, and Grattan DR. STAT5b is required for GH-induced liver IGF-I gene expression. *Endocrinology* 142: 3836–3841, 2001.
- Diehl KH, Hull R, Morton D, Pfister R, Rabemampianina Y, Smith D, Vidal JM, and vandeVorstenbosch C. A good practice guide to the administration of substances and removal of blood, including routes and volumes. *J Appl Toxicol* 21: 15–23, 2001.
- Febbraio MA and Pedersen BK. Muscle-derived interleukin-6: mechanisms for activation and possible biological roles. *FASEB J* 16: 1335–1347, 2002.
- Frank SJ. Growth hormone signaling and its regulation: preventing too much of a good thing. *Growth Horm IGF Res* 11: 201–212, 2001.
- Garcia-Martinez C, Llovera M, Agell N, Lopez-Soriano FJ, and Argiles JM. Ubiquitin gene expression in skeletal muscle is increased during sepsis: involvement of TNF- α but not IL-1. *Biochem Biophys Res Commun* 217: 839–844, 1995.
- Goodman MN. Interleukin-6 induces skeletal muscle protein breakdown in rats. *Proc Soc Exp Biol Med* 205: 182–185, 1994.
- Gornall AG, Bardawill CJ, and David MM. Determination of serum proteins by means of the biuret reaction. *J Biol Chem* 177: 751–766, 1949.
- Greenhalgh CJ, Metcalf D, Thaus AL, Corbin JE, Uren R, Morgan PO, Fabri LJ, Zhang JG, Martin HM, Willson TA, Billestrup N, Nicola NA, Baca M, Alexander WS, and Hilton DJ. Biological evidence that SOCS-2 can act either as an enhancer or suppressor of growth hormone signaling. *J Biol Chem* 277: 40181–40184, 2002.
- Grimble RF. Inflammatory response in the elderly. *Curr Opin Clin Nutr Metab Care* 6: 21–29, 2003.
- Haddad F and Adams GR. Acute cellular and molecular responses to resistance exercise. *J Appl Physiol* 93: 394–403, 2002.
- Haddad F and Adams GR. Inhibition of MAP/ERK kinase prevents IGF-I induced hypertrophy in rat muscles. *J Appl Physiol* 96: 203–210, 2004.
- Hashemolhosseini S, Nagamine Y, Morley SJ, Desrivieres S, Mercep L, and Ferrari S. Rapamycin inhibition of the G1 to S transition is mediated by effects on cyclin D1 mRNA and protein stability. *J Biol Chem* 273: 14424–14429, 1998.
- Heinrich PC, Behrmann I, Haan S, Hermanns HM, Muller-Newen G, and Schaper F. Principles of IL-6-type cytokine signaling and its regulation. *Biochem J* 374: 1–20, 2003.
- Hong-Brown LQ, Brown CR, Cooney RN, Frost RA, and Lang CH. Sepsis-induced muscle growth hormone resistance occurs independent of STAT5 phosphorylation. *Am J Physiol Endocrinol Metab* 285: E63–E72, 2003.
- Kawasome H, Papst P, Webb S, Keller GM, Johnson GL, and Gelfand EW. Targeted disruption of p70s6k defines its role in protein synthesis and rapamycin sensitivity. *Proc Natl Acad Sci USA* 95: 5033–5038, 1998.
- Kile BT and Alexander WS. The suppressors of cytokine signaling (SOCS). *Cell Mol Life Sci* 58: 1627–1635, 2001.
- Labarca C and Paigen K. A simple, rapid, and sensitive DNA assay procedure. *Anal Biochem* 102: 344–352, 1980.
- Lang CH, Fan J, Coney R, and Vary TC. IL-1 receptor antagonist attenuates sepsis-induced alterations in the IGF system and protein synthesis. *Am J Physiol Endocrinol Metab* 270: E340–E347, 1996.

36. Lieskovska J, Guo D, and Derman E. IL-6-overexpression brings about growth impairment potentially through a GH receptor defect. *Growth Horm IGF Res* 12: 388–398, 2002.
37. Lieskovska J, Guo D, and Derman E. Growth impairment in IL-6-overexpressing transgenic mice is associated with induction of SOCS3 mRNA. *Growth Horm IGF Res* 13: 26–35, 2003.
38. Ling PR, Schwartz JH, and Bistrrian BR. Mechanisms of host wasting induced by administration of cytokines in rats. *Am J Physiol Endocrinol Metab* 272: E333–E339, 1997.
39. Nemet D, Oh Y, Kim HS, Hill M, and Cooper DM. Effect of intense exercise on inflammatory cytokines and growth mediators in adolescent boys. *Pediatrics* 110: 681–689, 2002.
40. Olwin BB and Hauschka SD. Cell surface fibroblast growth factor and epidermal growth factor receptors are permanently lost during skeletal muscle terminal differentiation in culture. *J Cell Biol* 107: 761–769, 1988.
41. Ostrowski K, Rohde T, Schjerling P, Asp S, and Pedersen BK. Pro- and anti-inflammatory cytokine balance in strenuous exercise in humans. *J Physiol* 515: 287–291, 1999.
42. Pedersen BK, Steensberg A, Fischer C, Keller C, Keller P, Plomgaard P, Febbraio M, and Saltin B. Searching for the exercise factor: is IL-6 a candidate? *J Muscle Res Cell Motil* 24: 113–119, 2003.
43. Pedersen M, Bruunsgaard H, Weis N, Hendel HW, Andreassen BU, Eldrup E, Dela F, and Pedersen BK. Circulating levels of TNF- α and IL-6-relation to truncal fat mass and muscle mass in healthy elderly individuals and in patients with Type-2 diabetes. *Mech Ageing Dev* 124: 495–502, 2003.
44. Scheett TP, Nemet D, Stoppani J, Maresh CM, Newcomb R, and Cooper DM. The effect of endurance-type exercise training on growth mediators and inflammatory cytokines in pre-pubertal and early pubertal males. *Pediatr Res* 52: 491–497, 2002.
45. Schwartz J, Huo JS, and Pwien-Pilipuk G. Growth hormone regulated gene expression. *Minerva Endocrinol* 27: 231–241, 2002.
46. Solaro J, Pang DC, and Briggs FN. The purification of cardiac myofibrils with Triton X-100. *Biochim Biophys Acta* 245: 259–262, 1971.
47. Starr R and Hilton DJ. Negative regulation of the JAK/STAT pathway. *Bioessays* 21: 47–52, 1999.
48. Steensberg A, Febbraio MA, Osada T, Schjerling P, van Hall G, Saltin B, and Pedersen BK. Interleukin-6 production in contracting human skeletal muscle is influenced by pre-exercise muscle glycogen content. *J Physiol* 537: 633–639, 2001.
49. Steensberg A, Keller C, Starkie RL, Osada T, Febbraio MA, and Pedersen BK. IL-6 and TNF- α expression in, and release from, contracting human skeletal muscle. *Am J Physiol Endocrinol Metab* 283: E1272–E1278, 2002.
50. Takahashi T, Fukuda K, Pan J, Kodama H, Sano M, Makino S, Kato T, Manabe T, and Ogawa S. Characterization of insulin-like growth factor-I-induced activation of the JAK/STAT pathway in rat cardiomyocytes. *Circ Res* 85: 884–891, 1999.
51. Thomas G and Hall MN. TOR signaling and control of cell growth. *Curr Opin Cell Biol* 9: 782–787, 1997.
52. Tsika RW, Herrrick RE, and Baldwin KM. Interaction of compensatory overload and hindlimb suspension on myosin isoform expression. *J Appl Physiol* 62: 2180–2186, 1987.
53. Van der Meer MJM, Sweep CGJ, Rijnkels CEM, Pesman GJ, Tilders FJH, Kloppenborg PWC, and Hermus ARMM. Acute stimulation of the hypothalamic-pituitary-adrenal axis by IL-1 β , TNF α and IL-6: a dose response study. *J Endocrinol Invest* 19: 175–182, 1996.
54. Woelfle J and Rotwein P. In vivo regulation of growth hormone-stimulated gene transcription by STAT5b. *Am J Physiol Endocrinol Metab* 286: E393–E401, 2004.
55. Wright C, Haddad F, Qin A, and Baldwin KM. Analysis of myosin heavy chain mRNA expression by RT-PCR. *J Appl Physiol* 83: 1389–1396, 1997.
56. Yamauchi T, Kaburagi Y, Ueki K, Tsuji Y, Stark GR, Kerr IM, Tsushima T, Akanuma Y, Komuro I, Tobe K, Yazaki Y, and Kad-owaki T. Growth hormone and prolactin stimulate tyrosine phosphorylation of insulin receptor substrate-1, -2, and -3, their association with p85 phosphatidylinositol 3-kinase (PI3-kinase), and concomitantly PI3-kinase activation via JAK2 kinase. *J Biol Chem* 273: 15719–15726, 1998.
57. Zong C, Chan J, Levy DE, Horvath C, Sadowski HB, and Wang L. Mechanism of STAT3 activation by insulin-like growth factor I receptor. *J Biol Chem* 275: 15099–15105, 2000.

